KSCE Journal of Civil Engineering (2016) 20(6):2308-2318
DOI 10.1007/s12205-015-0267-6

Geotechnical Engineering
pISSN 1226-7988, eISSN 1976-3808
www.springer.com/12205

Intermittent Geofoam In-filled Trench for Vibration Screening Considering Soil Non-Linearity

Mainak Majumder* and Priyanka Ghosh**

Received April 4, 2015/Revised August 16, 2015/Accepted September 13, 2015/Published Online November 18, 2015

Abstract

The application of open as well as in-filled trenches as vibration screening technique has been considered in several situations. However, very few works have included the Expanded Polystyrene (EPS) geofoam as an in-filled material for the trench. The current study focuses on the effectiveness of the intermittent geofoam in-filled trench as vibration barrier in presence of machine induced ground vibration, where the geofoam blocks and the open air pockets are arranged alternately to form an effective vibration screening material. The screening efficiency of the geofoam in-filled trench is determined in terms of Amplitude Reduction Factor (ARF). The effect of the soil non-linearity under the propagating waves is also emphasized in the present study. Hyperbolic non-linear elastic Duncan and Chang (1970) soil model has been implemented in time domain finite element analysis. A parametric study is performed considering the geometric parameters of trench, excitation frequency, and stiffness of the soil.

Keywords: *Geofoam, vertical displacement, vibration screening, amplitude reduction factor, non-linear elastic, machine foundation*

1. Introduction

In recent times, rapid urbanization coupled with scarcity of land forces several industrial projects to come up ever closer to various civil engineering structures such as residential and office buildings, important heritage structures etc. sometime causing severe damage to the adjacent structures from both strength and serviceability point of view due to the operation of huge industrial machines producing unpleasant situation for the inhabitants such as unnecessary vibration, shaking etc. and also interrupting the operation of nearby sensitive equipments. The effect of such unwanted ground vibrations on the surrounding structures can be minimized by adopting various techniques such as changing the position of the source from the affected area, modifying the attenuation characteristics of the soil, using wave barriers, or using some damping devices in the form of base isolation (Celebi *et al.*, 2009). However, properly designed active wave barriers like trenches can reduce such machine induced vibrations significantly as well as economically since the frequency associated with the machine foundations is generally not very large as compared to other vibrating sources like earthquake (Kumar and Ghosh, 2006), blasting etc.

Trenches can be installed in different form like open or in-filled trenches (Woods, 1968; Richart *et al.,* 1970; Segol *et al.*, 1978; Haupt, 1981; Beskos *et al.*, 1986; Dasgupta *et al.,* 1990; Ahmad and Al-Hussaini, 1991; Saikia and Das, 2014) rows of piles (Liao and Sangrey, 1978; Kattis *et al.*, 1999; Tsai *et al.*, 2008), gas membranes (Massarsch, 2005). However, the usage of EPS geofoam as in-filled trench material in vibration screening technique is limited (Wang *et al.*, 2006; Alzawi and El Naggar, 2009; Murillo *et al.*, 2009). Due to very low acoustic impedance, geofoam can be used as an effective wave barrier in a trench. Davies (1994) has carried out centrifuge tests on nearby-buried structures using geofoam wave barriers, concrete walls and their composites, and concluded that well-designed geofoam barrier could largely reduce the magnitude of underground explosions on buried structures. Wang *et al.* (2009) have studied the use of geofoam barriers for the protection of buried structures from the blast-induced ground shock considering the barrier dimensions as per the prototype dimensions as proposed by Davies (1994). It has been reported that the geofoam barrier can provide flexibility in the design as well as in the screening efficiency. Murillo *et al.* (2009) have explored the application of geofoam in-filled barrier in reduction of the traffic induced vibrations. Alzawi and El Naggar (2011) have considered different configurations of geofoam in-filled walls such as single continuous, box wall, staggered wall to study the screening efficiency of geofoam in-filled barrier. Ekanayake *et al.* (2014) have analyzed the effect of water and EPS geofoam in-filled barrier. Recently, Majumder and Ghosh (2014) have performed numerical investigation of the vibration screening efficiency of continuous geofoam in-filled trench using two-dimensional finite element method. All the available studies related to geofoam as wave barrier have revealed that the geofoam in-filled barriers can be quite effective

*Research Scholar, Dept. of Civil Engineering, Indian Institute of Technology, Kanpur 208016, India (E-mail: mainakm@iitk.ac.in)
**Associate Professor, Dept. of Civil Engineering, Indian Institute of Technology, Kanpur 208016, India (Corresponding Author, E-mail: priyog@iitk.ac.in)

in screening of ground vibrations. However, geofoam being a costly material may not be economical if it is used in greater quantity in longer and deeper trenches. Keeping both cost and screening efficiency issues in mind, an innovative screening technique with intermittent geofoam in-filled trench is proposed in the present study. This method can be effectively adopted in the field as it satisfies the criteria of unsupported vertical depth of soil and also provides higher screening efficiency well comparable to that obtained by the open trench. In the analysis, two-dimensional finite element method is considered for the plane strain loading condition under dynamic mode. The soil is assumed to be isotropic, non-linear elastic material under the wave propagation. It is well understood fact that the soil behavior, in general, exhibits non-linear stress-strain variation under different loading conditions; however, the developed strain may or may not reach the limiting/ultimate condition. Hence, in the present study a special attention is given to the soil non-linearity and its effect on the screening efficiency of intermittent geofoam in-filled trench by varying the geometry of the trench, the excitation frequency, and the inclination of the trench. A detailed parametric study has been performed to investigate the performance and effectiveness of proposed intermittent geofoam in-filled trench as the vibration barrier.

2. Problem Definition

A rigid embedded strip foundation subjected to a vertical dynamic load intensity of $p(t) = p_0 sin(\omega t)$ is considered in the study. The foundation is placed on dry, non-linear elastic, homogeneous and non-homogeneous soil deposits with an embedment factor (D_f/B) of 1.0. The foundation is expected to carry a static working load causing uniform static load intensity on the foundation without violating the ultimate state. One-side trench of depth, d and width, w is placed at a center-to-center distance of l from the foundation as shown in Fig. 1. The objective is to determine the active vibration screening efficiency of intermittent geofoam in-filled trench in terms of Amplitude Reduction Factor (ARF) by measuring the reduction in the displacement amplitude at different pick up points caused by the sinusoidal dynamic excitation on the foundation. The *ARF* can be expressed as (Woods, 1968)

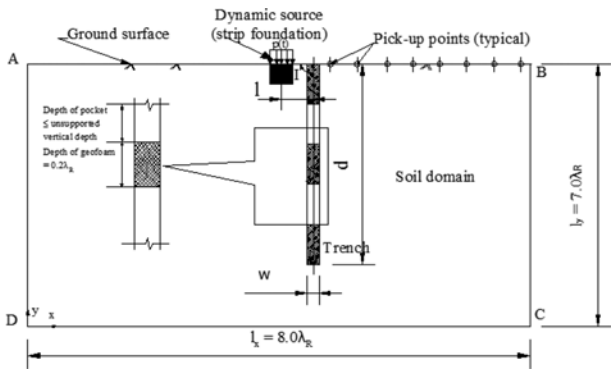

Fig. 1. Schematic Diagram of Finite Element Soil Domain and Trench Geometric Parameters

$$ARF = \frac{(U_v)_{After}}{(U_v)_{Before}} \tag{1}$$

where, $(U_v)_{Before}$ and $(U_v)_{After}$ are the vertical displacement at any pick up point before and after installation of the trench, respectively. The *ARF* values are calculated by considering the peak displacement amplitude of the dynamic response, which is discussed thoroughly in section 4.

3. Analysis

3.1 Non-linear Soil Model

In the present study, the soil deposit is assumed to obey Duncan and Chang (DC) non-linear hyperbolic elastic model (Duncan and Chang, 1970), whereas the geofoam is modeled as linear elastic material. The DC hyperbolic non-linear elastic model is reported as an effective soil model which is capable to capture the soil non-linearity efficiently and can be expressed as:

$$\sigma_1 - \sigma_3 = \frac{\varepsilon}{\frac{1}{E_i} + \frac{\varepsilon}{(\sigma_1 - \sigma_3)_{ult}}} \tag{2}$$

Where, $(\sigma_1 - \sigma_3)_{ult}$ is the ultimate deviatoric stress.

Different parameters involved in the DC model can be obtained by performing triaxial test. The stress-strain relationship of the DC model has been already reported by Duncan and Chang (1970), where the asymptotic value of $(\sigma_1 - \sigma_3)$ i.e. the ultimate deviatoric stress is found to be larger than the compressive strength, $(\sigma_1 - \sigma_3)_f$ of the soil and the hyperbolic curve remains below the asymptote, where $(\sigma_1 - \sigma_3)_f$ is the deviatoric stress at the failure. The values of the deviatoric stress at the failure and at the ultimate state are correlated with the factor R_f or the failure ratio and can be written as:

$$R_f = \frac{(\sigma_1 - \sigma_3)_f}{(\sigma_1 - \sigma_3)_{ult}} \tag{3}$$

As per Janbu (1963), the stress dependent initial tangent modulus can be determined based on the minor principal stress and can be expressed as:

$$E_i = TP_a\left(\frac{\sigma_3}{P_a}\right)^n \tag{4}$$

Where T and n are the dimensionless material parameters termed as modulus number and modulus exponent, respectively.

If the minor principal stress remains unchanged, mathematically the initial tangent modulus at any point may be derived by differentiating the deviatoric stress (Eq. (2)) with respect to the axial strain, ε and can be given by

$$E_i = \frac{\partial(\sigma_1 - \sigma_3)}{\partial \varepsilon} \tag{5}$$

After differentiating and simplifying, the tangent modulus can

be obtained as

$$E_t = (1 - R_f SL)^2 \times E_i \quad (6)$$

Where, SL is the stress level and can be expressed as

$$SL = \frac{(\sigma_1 - \sigma_3)}{(\sigma_1 - \sigma_3)_f}$$

Based on the experimental results, Duncan and Chang (1970) have also proposed the unloading-reloading state, where the soil behaves nearly elastically. The magnitude of unloading-reloading modulus is also dependent on the confining pressure and the relation is similar to that reported by Janbu (1963).

$$E_{ur} = T_{ur} P_a \left(\frac{\sigma_3}{P_a}\right)^n \quad (7)$$

3.2 Materials

To incorporate the non-linear elastic DC soil model, two different homogeneous soil deposits (deposit-A and deposit-B) have been considered in the analysis as proposed by Shen *et al.* (1981) based on the undrained triaxial test data and the different model parameters required for the non-linear analysis as well as the soil properties are given in Tables 1 and 2, respectively. A non-homogeneous layered soil deposit (deposit-C) has also been considered to explore the effect of the stiffness variation on the screening efficiency. Deposit-C consists of the top half made of softer deposit, deposit-A and the bottom half made of deposit-B. The different properties of deposit-C are listed in Table 3. The magnitude of E_i in the DC model is dependent on the confining pressure and other model parameters as expressed in Eq. (4). However, in case of dynamic analysis, a preliminary guess for the domain size needs to be initiated to know the initial modulus and wave velocities. However, the domain size cannot be fixed without knowing the value of wavelength. Therefore, the initial value of the shear wave velocity of the soil deposit has been determined based on the empirical relation reported for the sandy soil (Phuoc, 2008)

$$T = \frac{\rho V_s^2 (1 + \upsilon)}{P_a} \quad (8)$$

The shear wave velocity, V_s can be calculated from Eq. (8) by putting the values of different parameters for two different deposits as given in Table 2. Having fixed the domain size in the deposit-A the major and minor principal stresses turn out to be 691.71 kN/m^2 and 196.38 kN/m^2, respectively. Subsequently, the magnitude of the initial tangent modulus (E_{is}) under static condition can be derived as 1.77×10^4 kN/m^2 from Eq. (4). Similarly, for deposit-B the magnitude of E_{is} is found to be 8.82×10^4 kN/m^2. The other dynamic properties of two different deposits are listed in Table 4. The change in the initial tangent modulus of the soil deposits under dynamic condition is determined by following the theory reported by Alpan (1970). The initial tangent modulus (E_{id}) under dynamic condition corresponding to that under static condition is determined from the empirical curves proposed by Alpan (1970) and the modified values of E_{id} for different deposits are given in Table 4. Alpan (1970) has proposed that in cohesive as well as granular soil, the ratio of dynamic to static stiffness increases with a decrease in the vibration period particularly under dry condition due to the densification occurs during dynamic loading/shaking. The effect of the water table is not taken into consideration in the study. The embedded concrete foundation has the bulk and the shear modulus of 1.39×10^7 kN/m^2 and 1.04×10^7 kN/m^2, respectively.

In the present study, EPS geofoam is considered to model the vibration barrier, which is pretty light weight geosynthetic material. As discussed earlier, the application of EPS geofoam as vibration screening material has not been explored as much as other applications are studied such as lightweight fill material, compressible inclusions and thermal insulation material. As per ASTM D6817, the available density of EPS geofoam varies

Table 1. DC Model Parameters used in the Analysis (Shen *et al.*, 1981)

Properties	Deposit-A (Sandy silt)	Deposit-B (Sandy clay)
Modulus exponent (n)	0.84	0.60
Modulus number (K)	100	280
Unloading-reloading coefficient (K_{ur})	300	840
Failure ratio (R_f)	0.77	0.93

Table 2. Soil Properties used for Non-linear DC Model (Shen *et al.*, 1981)

Properties	Deposit-A (Sandy silt)	Deposit-B (Sandy clay)
Dry unit weight, γ_{dry} (kN/m^3)	19.06	19.06
Undrained cohesion, c_u (kN/m^2)	51.71	87.15
Angle of internal friction, ϕ (^{o})	27	18
Poisson's ratio, υ	0.3	0.3

Table 3. Material Properties of Deposit-C (non-homogeneous)

Properties	
Equivalent undrained cohesion, $c_{u,eq}$ (kN/m^2)	69.43
Equivalent angle of internal friction, ϕ_{eq} (^{o})	22.64
Equivalent dry unit weight of soil, γ_{dry} (kN/m^3)	19.35

Table 4. Dynamic Properties of Different Soil Deposits

Properties	Deposit-A (Sandy silt)	Deposit-B (Sandy clay)
Initial static elastic modulus, E_{is} (kN/m^2)	1.77×10^4	8.82×10^4
Initial dynamic elastic modulus, E_{is} (kN/m^2)	1.86×10^4	8.89×10^4
Dynamic Shear modulus, G (kN/m^2)	7.15×10^3	34.20×10^3
Shear wave velocity, V_s (m/s)	61.26	132.19
Longitudinal wave velocity, V_P (m/s)	114.62	247.29
Rayleigh wave velocity, V_R (m/s)	56.79	122.54
Rayleigh wavelength, $\lambda_R = V_R/F$ corresponding to F = 5 Hz	11.36	24.51
Acoustic impedance, Z_s (kN-s/m^3)	218.47	483.95
Rayleigh damping coefficient, α	0.059	0.058
Rayleigh damping coefficient, β	0.026	0.025

from 11.2 kg/m^3 (EPS12) to 45.7 kg/m^3 (EPS46). It has been revealed from earlier works (Celebi and Schmid, 2005; Babu *et al.,* 2011) that in the vibration screening method, the material with lower stiffness and density may serve as an efficient alternative of practically infeasible open trench. In the present analysis, EPS12 is considered as in-filled material, which has elastic modulus and Poisson's ratio of 3.3 MPa and 0.1, respectively. It is worth noting that due to very low stiffness value, the geofoam may squeeze under large confining pressure offered by surrounding soil, which may be prevented by providing some lateral stiffener during the installation process. However, the installation and serviceability aspects of the intermittent geofoam in-filled trench in the field are beyond the scope of the present study. The acoustic impedance of EPS12 is determined as Z_G = 7.72 kN-s/m^3 which is found to be significantly lower than that of different soil deposits as given in Table 4. The large difference in the acoustic impedance between soil and geofoam results in less transfer of energy from one medium to another and thus creating better environment for vibration screening.

3.3 Dynamic and Static Loading on Foundation

A constant amplitude sinusoidal dynamic vertical excitation has been applied on the foundation. However, at a very low magnitude of dynamic loading, the soil non-linearity is not expected to get developed due to significantly small strain level. Therefore, the values of the shear strain have been obtained at different pick-up points along the ground surface (x/λ_R = 1.65, 1.75, 1.85, 5.00) to determine the magnitude of P_0 at which the soil non-linearity gets developed. Soil generally exhibits linear elastic behavior up to a shear strain (γ) level of 10^{-3}% (Kramer, 1996). The variation of shear strain with the magnitude of P_0 is shown in Fig. 2. It can be seen that beyond P_0 = 5 kN the shear strain at the selected pick-up points exceeds the threshold limit of linear elastic behavior. Therefore, a vertical sinusoidal loading with an amplitude of 5 kN and a loading time of 10 seconds has been applied on the machine foundation. In addition, a static working load intensity of 10 kN/m^2 is considered on the foundation as the self-weight of the machine and other accessories. The magnitude of total vertical loading has been compared with the ultimate bearing capacity of each deposit, which is found to be significantly higher than the applied loading on the foundation and thus, ensuring no plastic deformation in the soil under dynamic condition. Further, by following the recommendation of Kramer (1996), the magnitude of the resonant frequency of each layer for constant force type machine excitation is determined as 0.58 Hz. Therefore, considering low-speed machine and the criteria to avoid resonance, the operating frequency of the machine is selected as 5 Hz.

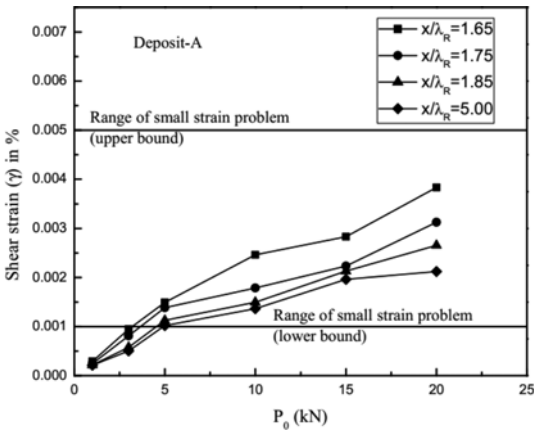

Fig. 2. Variation of Shear Strain with P_0 at Different Pick-up Points

3.4 Finite Element Modeling

The influence domain is discretized with six-noded triangular elements using *PLAXIS V8.5* (Plaxis 2002), which are found to generate fairly accurate solution in standard deformation problems. The problem in hand satisfying the plane strain condition associated with strip loading with trench on one side is analyzed with full domain as shown in Fig. 3. Non-linear elastic model is not available in *PLAXIS* and therefore, the DC non-linear elastic hyperbolic model has been included through the option of user defined soil model available in *PLAXIS*. The computer code for DC model has been written in *FORTRAN* and compiled in the available dynamic link library format. The implementation of

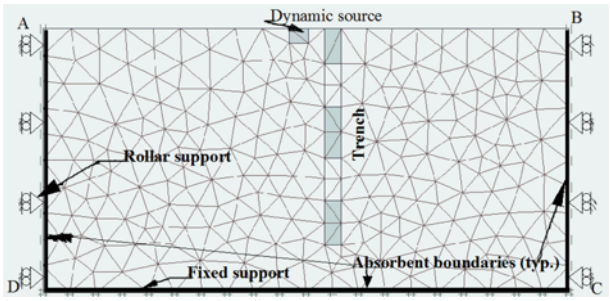

Fig. 3. Finite Element Discretization and Boundary Conditions for Influence Domain

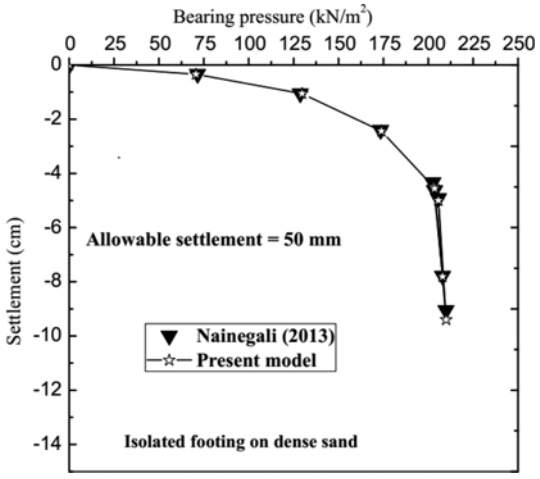

Fig. 4. Validation of Present Study with Nainegali (2013) using DC Model under Static Condition

DC model in *PLAXIS* has been validated under static condition by analyzing an isolated strip footing of 1 m width resting on dense sand whose properties have been reported by Duncan and Chang (1970). In Fig. 4, the load-settlement plot obtained from the present analysis for isolated strip footing is compared with that reported by Nainegali (2013) using DC model and a perfect match can be observed which virtually authenticates the correctness of the present non-linear analysis. Sensitivity analysis has been carried out to determine the depth of influence domain by considering the average displacements along the vertical side boundary (BC in Fig. 1) of the domain (ABCD) as well as the displacement at the base of the footing normalized with respect to the Rayleigh wavelength, λ_R (Fig. 1) for all deposits. The value of λ_R for deposit-A and deposit-B corresponding to 5 Hz frequency is mentioned in Table 4. The magnitude of λ_R for deposit-C is found to be 15.52 m at 5 Hz frequency, which is computed taking the contribution of different layers. The average displacement along the vertical boundary is obtained by averaging the displacements recorded along BC at an interval of $0.1\lambda_R$. The optimum depth of the domain is determined by keeping the domain size as $2.5\lambda_R$ in the horizontal (x) direction. It can be seen from Fig. 5 that beyond the depth of $7.0\lambda_R$ the average displacement along the vertical side boundary (BC) as well as the total displacement at the base of the footing remain almost constant and hence, the domain size is assumed as $7.0\lambda_R$ along the vertical direction. After fixing the optimum domain depth, sensitivity analysis has been performed to fix the domain size along the horizontal direction. Fig. 6 depicts that beyond the width of $8.0\lambda_R$ the average displacement along BC remains almost unchanged and hence, the domain size is assumed as $8.0\lambda_R$ along x direction. Total fixities are applied at the base of the model, whereas horizontal fixities are applied at the extreme vertical boundaries restraining the motion along the horizontal direction as shown in Fig. 3. In addition, the absorbent boundary condition is considered at the extreme boundaries (AD, BC and CD) to absorb the increment of stresses on the boundaries caused by the dynamic loading and to avoid the reflection of waves back to the soil body as described by Lysmer and Kuhlmeyer (1969). The average element size ($0.121\lambda_R$) is chosen by satisfying the criteria of wave propagation as proposed by Kramer (1996). The total dynamic excitation time is considered as 10 seconds, where the time step considered in the present dynamic analysis satisfies the following criteria (Valliappan and Murti, 1984)

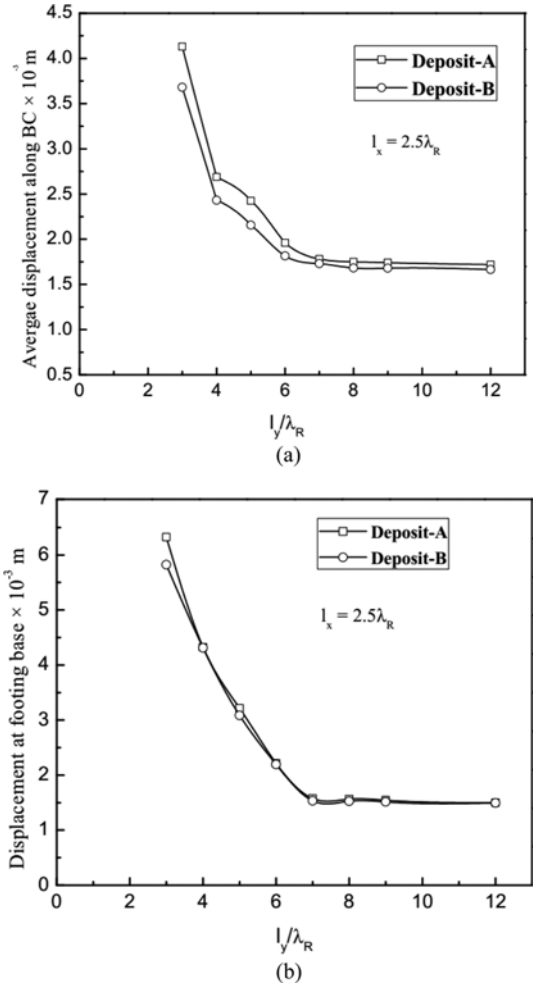

Fig. 5. Sensitivity analysis for Domain Size Along Vertical Direction Considering: (a) Average Displacement Along BC, (b) Displacement at Footing Base

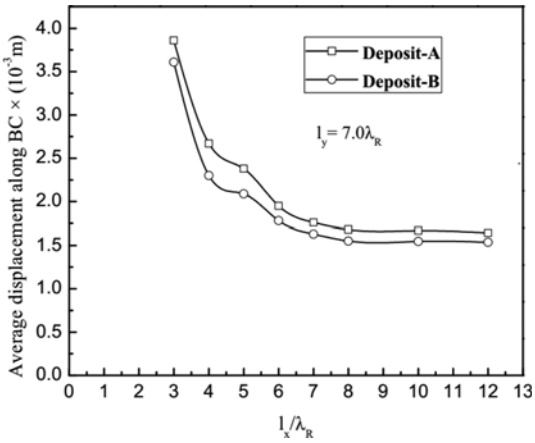

Fig. 6. Sensitivity Analysis for Domain Size Along Horizontal Direction (l_x)

$$\Delta t \leq \frac{Average\ \ element\ \ size}{Velocity\ \ of\ \ slowest\ \ propagating\ \ wave} \tag{9}$$

The damping is an important factor influencing the dynamic analysis significantly. In a soil deposit, the material damping is generally caused by its viscous properties, friction and the development of plasticity. The damping ratio (ξ) of 5-8% is quite common in the vibration screening problem (Al-Hussaini and Ahmad, 1996; Alzawi and El Naggar, 2009; Di Mino *et al*., 2009) and in the present analysis the magnitude of ξ is assumed as 6% for all deposits. In the analysis, Rayleigh damping is assumed for simulating such viscous damping, which is proportional to the mass and stiffness of the system and can be defined as:

$$[C] = \alpha[M] + \beta[K] \quad (10)$$

where, α and β are the Rayleigh damping coefficients, where α and β determine the influence of the mass and the stiffness in the damping of the system, respectively. The values of Rayleigh damping coefficients (α and β) can be evaluated by choosing 1st and 2nd natural frequency (f_1 and f_2) of the soil deposit. The magnitudes of α and β for deposit-A and -B are determined by following the procedure described by Di Mino *et al.* (2009) for ξ = 6% and are given in Table 4, whereas for deposit-C, the Rayleigh damping coefficients α and β are found to be 0.059 and 0.026, respectively.

3.5 Concept of Intermittent Geofoam In-filled Trench

The present investigation mainly focuses on the application of intermittent geofoam (*IF*) as the vibration barrier (Fig. 1). The concept of *IF* is proposed based on the fact that the vibration screening efficiency obviously increases by lowering the acoustic impedance of in-filled material in the trench. Therefore, in this study a combination of void space (air pocket) and geofoam arranged alternately is used throughout the depth of the trench to obtain better screening efficiency. The alternate arrangement of geofoam and empty pockets as shown in Fig. 7 consumes less material, hence cost effective and at the same time provides comparable screening efficiency to that obtained from open trench which is rather practically infeasible. The height of each pocket along the depth of the trench is determined based on the concept of unsupported vertical cut in soil. Following the theory of classical soil mechanics the unsupported vertical height in soil is determined considering 40 kPa surcharge applied just beside the trench (worst possible case) on the ground surface caused by the self-weight of foundation as well as machine parts under static condition. The magnitude of unsupported vertical height determined for different deposits are found to be 6.75, 10.21 and 8.70 m for deposit-A, B and C respectively. By keeping the pocket height lesser or equal to the unsupported vertical depth, the intermittent geofoam is placed within the trench in three layers with a depth of $0.2\lambda_R$ for each layer (Fig. 7). It is worth noting here that the total volume ($0.03\lambda_R^3$) of geofoam is kept constant along the depth of the trench by varying the height of the void space without violating the concept of unsupported vertical depth. Hence, the present design philosophy imparts an economic but efficient vibration screening technique. Fig. 7 represents the details of geometry of the pockets as well as the intermittent geofoam used in the trench.

4. Results and Discussions

The non-linear analysis has been carried out to obtain the magnitude of *ARF* (Eq. (1)) at different pick-up points along the ground surface. The location of pick-up points along the ground surface is varied from 4.4 λ_R to 5.0 λ_R as shown in Fig. 1, with an interval of 0.1 λ_R. The pick-up points are chosen along the ground surface since the response captured at the ground surface is found to be maximum compared to anywhere in the domain due to the amplification of excitation. For F = 5 Hz, the peak vertical displacement amplitudes obtained at different pick-up points in different deposits without any trench are given in Table 5. It can be seen that the maximum value of peak vertical displacement amplitude for *no trench* condition is observed at x/λ_R = 4.5. The peak vertical displacement with intermittent or continuous geofoam in-filled trench can be obtained by multiplying corresponding *ARF* value with the values reported in Table 5 for different deposits.

A nomenclature $(L_i W_j D_K F_m I_n)_{IF/CF/OT}$ is considered in the present study to identify each problem and other associated details.

Where,

L_i : represents the location factor i.e. center to center distance between the footing and the trench normalized with respect to λ_R, where i stands for different magnitude of L = {0.15, 0.20, 0.25, 0.30}

Table 5. Peak Vertical Displacement Amplitude at Different Pick-up Points with F = 5 Hz in Different Deposits Without Trench

	Peak vertical displacement amplitude (mm)						
x/λ_R	4.4	4.5	4.6	4.7	4.8	4.9	5.0
Deposit-A	8.01	9.34	8.20	7.80	6.51	5.62	5.28
Deposit-B	6.12	8.10	5.61	4.39	4.14	3.81	3.51
Deposit-C	6.55	8.86	6.68	5.92	5.48	4.77	4.54

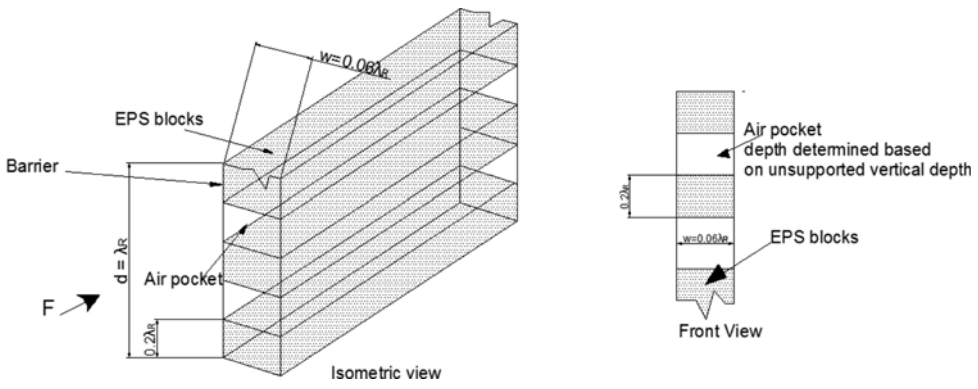

Fig. 7. Details of Geometry of Intermittent Geofoam (*IF*) in-filled Trench

W_j: represents the width factor of trench i.e. normalized width with respect to λ_R, where j stands for different magnitude of W = {0.04, 0.06, 0.08, 0.10}

D_k: represents the depth factor of trench i.e. normalized depth with respect to λ_R, where k stands for different magnitude of D = {0.8, 1.0, 1.2}

F_m: represents the excitation frequency of machine (in Hz), where m stands for different magnitude of F = {5, 10, 20, 30, 40, 50} Hz

I_n: represents the inclination of trench (in degrees), where n stands for different magnitude of I = {45, 60, 90}°

IF, CF, OT represent the intermittent geofoam in-filled trench, continuous geofoam in-filled trench and open trench, respectively. Whenever, the results obtained from the linear (*LE*) and non-linear analysis (*NL*) are presented together, the nomenclature is modified as $(L_i W_j D_K F_m I_n)^{LE/NL}_{IF/CF/OT}$. Since the deposit-A is found to be the softest, all the results are reported for deposit-A. However, all three deposits are considered only to study the stiffness effect on the screening efficiency. Having discussed the influence of trench geometry and other parameters on the *ARF* value considering soil non-linearity a comparative study has been performed between linear and non-linear analysis separately.

In Fig. 8, the variation of vertical displacement amplitude obtained for *IF* and *no trench* condition is shown for pick-up point at x/λ_R = 4.4. A significant reduction in the vertical displacement amplitude can be observed using intermittent geofoam in-filled trench. In Fig. 9, the variation of *ARF* at different pick up points in deposit-A is shown for intermittent geofoam with different trench locations keeping other parameters fixed such as W = 0.06, D = 1.0, F = 5 Hz, I = 90°. It can be seen from Fig. 9 that the magnitude of *ARF* decreases from 0.265 to 0.189 with decrease in L from 0.30 to 0.15 at x/λ_R = 4.7, which indicates the enhancement in the screening effectiveness with decrease in the distance between the source and the trench. It is worth noting that the range of location factor (L_i) needs to be selected based on the wavelength of the Rayleigh wave. In the analysis, no significant reduction in the *ARF* magnitude is observed beyond L = 0.15 and hence, the optimum location factor for the trench is considered as L = 0.15 to determine the effect of other input parameters on the required isolation efficiency. Fig. 10 shows the variation of *ARF* with the width of geofoam in-filled trench for *IF* in deposit-A keeping other parameters fixed such as L = 0.15, D = 1.0, F = 5 Hz, I = 90°. Woods (1968) has reported that the width of open trench does not play any significant role in the screening effectiveness. However, it can be seen that the screening efficiency increases (*ARF* decreases) with increase in geofoam width. This may be attributed to the longer travel path of the waves through a material (geofoam) with lesser acoustic impedance compared to soil. The magnitude of *ARF* is found to decrease from 0.213 to 0.181 with increase in W from 0.02 to 0.08 corresponding to the pick-up point at x/λ_R = 4.7. It is quite distinct from Fig. 10 that the improvement in *ARF* continues with increase in the width of geofoam up to a certain limit by sacrificing the cost-effectiveness of the design philosophy. However, depending on the commercial availability, an optimum width (W = 0.06) of geofoam is considered for the further analysis. The influence of the depth of trench on the variation of *ARF* is

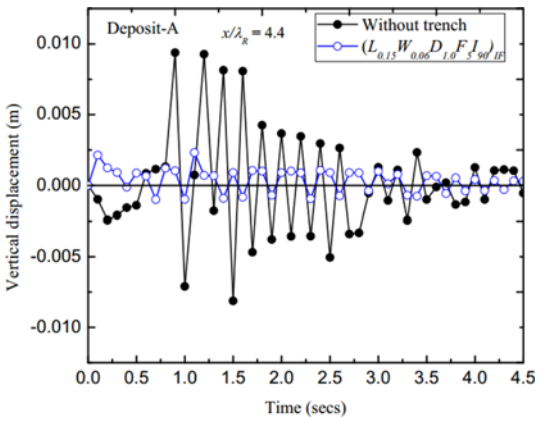

Fig. 8. Comparison of Vertical Displacement Amplitude between *IF* and *no trench* for Pick-up Point at x/λ_R = 4.4

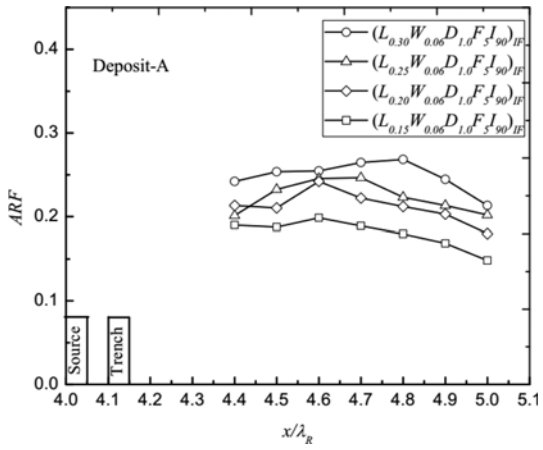

Fig. 9. Variation of *ARF* with Different Pick-up Points for Intermittent Geofoam with Different Trench Locations in Deposit-A

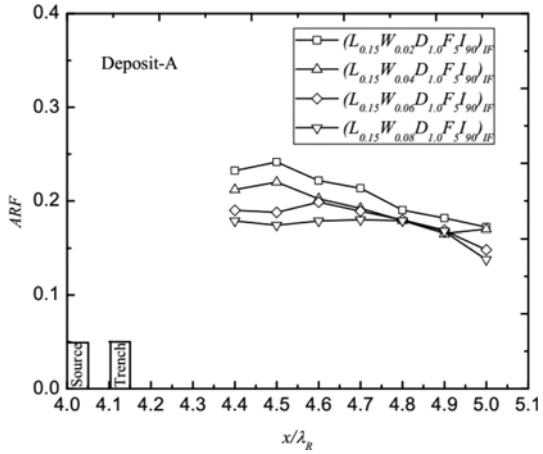

Fig. 10. Variation of *ARF* at Different Pick-up Points for Intermittent Geofoam with Different Trench Widths in Deposit-A

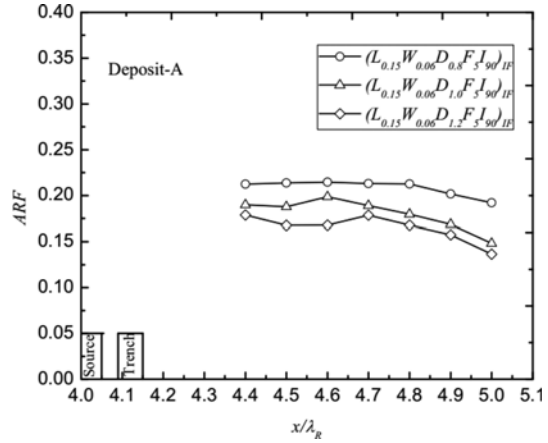

Fig. 11. Variation of *ARF* at Different Pick-up Points for Intermittent Geofoam with Different Trench Depths in Deposit-A

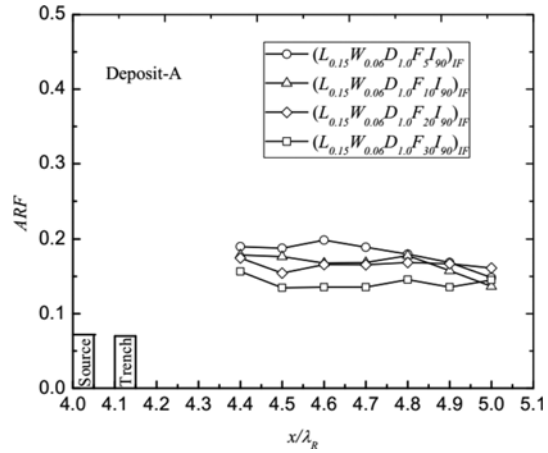

Fig. 12. Variation of *ARF* at Different Pick-up Points for Intermittent Geofoam at Different Frequency of Excitation in Deposit-A

presented in Fig. 11. It can be noted that the *ARF* value decreases from 0.213 to 0.179 with increase in the value of depth factor D from 0.8 to 1.2 with L = 0.15, W = 0.06, F = 5 Hz, I = 90° corresponding to the pick-up point at x/λ_R = 4.7. Significant reduction in the vibration amplitude occurs with increasing D due to delay in the arrival of the wave at the pick-up points and the depth of trench seems to be the most important parameter for such vibration screening problem. For *IF*, the variation of *ARF* at different pick-up points with different excitation frequencies is shown in Fig. 12. It can be observed that the magnitude of *ARF* decreases with increase in the excitation frequency of the vibrating source. In other words, higher the frequency smaller is the wavelength and hence there is an improvement in the screening efficiency. The *ARF* value decreases from 0.189 to 0.135 with increase in frequency, F from 5 Hz to 30 Hz corresponding to the pick-up point at x/λ_R = 4.7. The inclination (I) of trench is also varied in the analysis and the details are presented in Fig. 13. Keeping the concept of inclined reflector in mind the inclination of geofoam in-filled trench is varied from 45° (inclined) to 90° (vertical). The effect of the inclination of

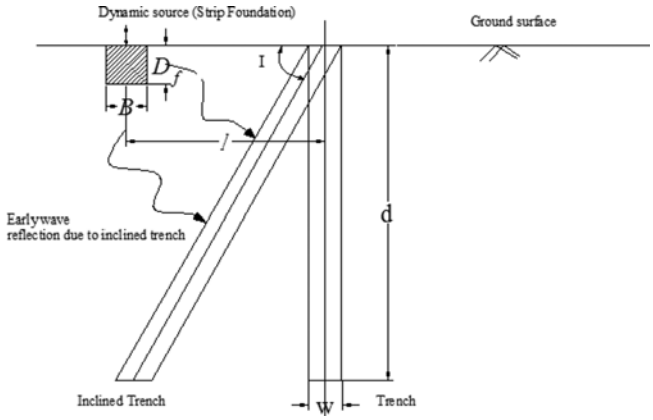

Fig. 13. Details of Inclined Trench

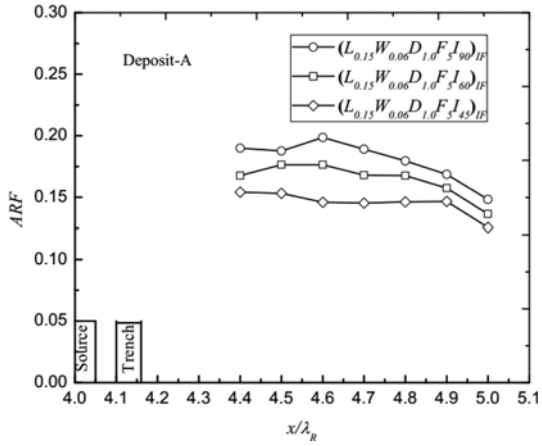

Fig. 14. Variation of *ARF* at Different Pick-up Points for Intermittent Geofoam with Different Trench Inclinations in Deposit-A

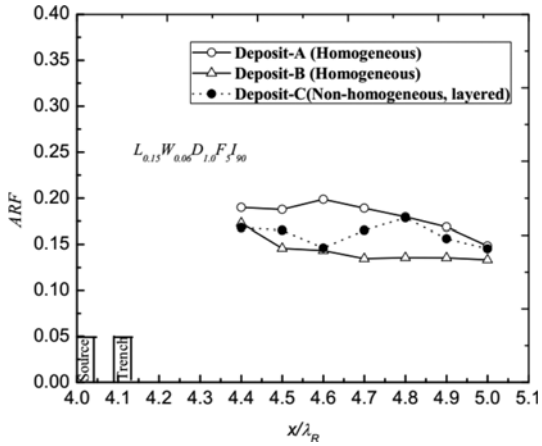

Fig. 15. Variation of *ARF* at Different Pick-up Points for Intermittent Geofoam in Different Deposits

trench on the *ARF* value is shown in Fig. 14. It can be noticed from Fig. 14 that the magnitude of *ARF* decreases with decrease in the inclination of trench from 90° to 45°. The amount of reduction in *ARF* with decrease in the inclination from 90° to 45° is found to be from 0.189 to 0.145. This may be attributed to a

significant amount of waves gets reflected from the inclined barrier as compared to that from the vertical one.

Above results are reported for deposit-A as it has got the lowest stiffness and therefore, is expected to be affected more critically under the vibration than other stiffer deposits. However, in Fig. 15 the variation of *ARF* is presented for different soil deposits to explore the effect of the stiffness of different deposits on the screening efficiency. It can be observed that the *ARF* value decreases from 0.189 to 0.165 with increase in the soil stiffness from deposit-A (homogeneous) to deposit-B (homogeneous) corresponding to the pick-up point at $x/\lambda_R = 4.7$.

5. Comparison

The vertical displacement response observed at the pick-up point, $x/\lambda_R = 4.4$ and the *ARF* values obtained for different trench conditions such as *OT*, *IF* and *CF* with $L = 0.15$, $W = 0.06$, $D = 1.0$, $F = 5$ Hz and $I = 90^o$ are compared in Fig. 16. It can be observed that the vertical displacement response as well as the *ARF* values obtained from *IF* are found to be significantly lower than those obtained from *CF*, whereas the results of *OT* are seen to be the lowest for obvious reason.

It is worth noting that the present analysis considers soil non-linearity under the wave propagation caused by moderately strong machine vibration, whereas the earlier studies available in the literature have mostly considered linear elastic soil medium to determine the screening efficiency of in-filled trenches. Hence, a comparison between non-linear and linear analysis is made to show that the linear analysis predicts conservative results (higher ARF) when the strain level crosses the lower bound as shown in Fig. 2, which virtually justifies the need of performing present non-linear analysis. In Fig. 17, the vertical displacement response observed at the nearest pick-up point, $x/\lambda_R = 4.4$ as well as the *ARF* values obtained from both linear and non-linear analysis are compared to understand the consequences of soil non-linearity on the screening efficiency of intermittent geofoam in-filled trench. From Fig. 17(a), the peak vertical displacement amplitude is found to decrease considerably from 4.28 mm (linear) to 2.38 mm (non-linear) at the nearest pick-up point, $x/\lambda_R = 4.4$ for $L = 0.15$, $W = 0.06$, $D = 1.0$, $F = 5$ Hz, $I = 90^o$. Considering soil non-linearity the magnitude of ARF decreases from that obtained from the linear analysis in the range of 0.212 to 0.189 for $L = 0.15$, $W = 0.06$, $D = 1.0$, $F = 5$ Hz, $I = 90^o$.

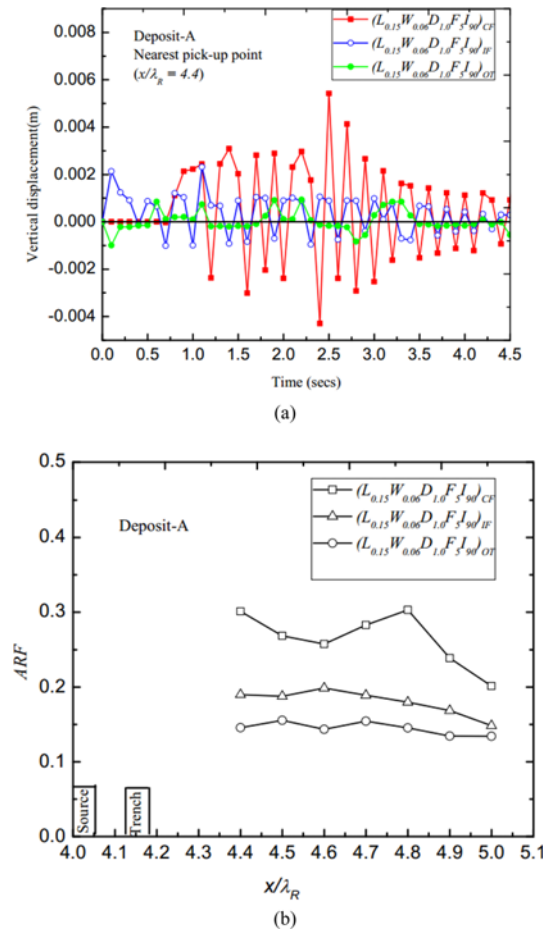

Fig. 16. Comparison of: (a) Vertical Displacement Response, (b) *ARF* for Different Trench Conditions in Deposit-A

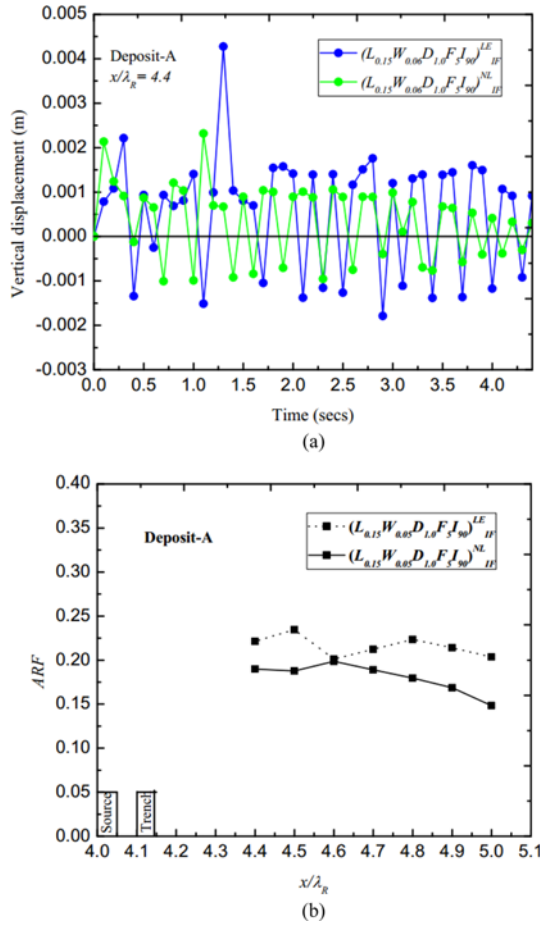

Fig. 17. Comparison of: (a) Vertical Displacement Response, (b) *ARF* for Linear and Non-linear Analysis in Deposit-A

6. Conclusions

The present finite element analysis explores the possibility of vibration screening technique using intermittent geofoam in-filled trench in non-linear elastic soil medium. The effect of different parameters such as trench width, depth, inclination and location, frequency of excitation and soil stiffness on the *ARF* has been studied critically. Based on the scope of the present investigation, the following conclusions can be made:

1. A significant reduction in *ARF* can be achieved by considering *IF* over *CF*. However, the screening efficiency of *IF* is found to be lesser than that obtained from *OT* for obvious reason.
2. For *OT* and *CF*, the key parameters are found to be the depth and location of the trench; whereas in case of *IF*, other than the depth of trench, the volume of air pockets plays an important role in the screening efficiency.
3. The intermittent geofoam in-filled trench with $D = 1.0$, $W = 0.06$ and $L = 0.15$ is found to be most effective from both screening efficiency and economic point of view.
4. The efficiency of *IF* increases with increase in the frequency of the vibrating source and therefore, *IF* is expected to be more effective for high frequency dynamic sources such as high-speed turbines, compressors, generators etc. Further, the screening efficiency of *IF* is found to increase with increase in the stiffness of the soil deposit.
6. Soil non-linearity significantly enhances the screening efficiency as compared to the linear elastic analysis available in the literature. The non-linear analysis reveals a reduction in the *ARF* value in the range of 0.212 to 0.189 as compared to that obtained from the linear analysis for $L = 0.15$, $W = 0.06$, $D = 1.0$, $F = 5$ Hz, $I = 90^{o}$.

Notaions

ARF = Amplitude reduction factor
B = Width of footing
c_u = Undrained cohesion of soil
$c_{u,eq}$ = Equivalent undrained cohesion of soil
$[C]$ = Damping matrix
d = Depth of trench
D = Depth factor for trench, d/λ_R
D_f = Depth of footing in soil
E_i = Initial tangent modulus
E_{is} = Initial tangent modulus under static condition
E_{id} = Initial tangent modulus under dynamic condition
E_t = Tangent modulus
E_{ur} = Unloading-reloading modulus
f_1, f_2 = 1st and 2nd natural frequency of soil deposit
F = Frequency of dynamic excitation
f_{eq} = Equivalent angle of internal friction
G = Shear modulus of soil
I = Inclination angle of trench
$[K]$ = Stiffness matrix
l = Center to center spacing between source and trench
L = Location factor for trench, l/λ_R
$[M]$ = Mass matrix
n = Dimensionless parameter
P_a = Atmospheric pressure
P_0 = Dynamic loading amplitude
p_0 = Constant amplitude of dynamic loading intensity
$p(t)$ = Dynamic loading intensity with constant amplitude
R_f = Failure ratio
SL = Stress level
T = Dimensionless parameter
T_{ur} = Dimensionless parameter
U_V = Vertical displacement
V_P = Longitudinal wave velocity of soil
V_R = Rayleigh wave velocity in soil
V_s = Shear wave velocity in soil
w = Width of the trench
W = Width factor for trench, w/λ_R
Z_G = Acoustic impedance of geofoam
Z_S = Acoustic impedance of soil
t = Time
λ_R = Rayleigh wavelength
α *and* β = Rayleigh damping coefficients
ε = Axial strain
ϕ = Angle of internal friction of soil
ρ = Density of soil
γ = Shear strain
γ_s = Unit weight of soil
γ_{dry} = Dry unit weight of soil
σ_1, σ_3 = Major and minor principal stress
ξ = Damping ratio
υ = Poisson's ratio of soil
ω = Circular frequency of vibration
Δt = Time step of dynamic analysis

References

Ahmad, S. and Al-Hussaini, T. M. (1991). "Simplified design for vibration screening by open and in-filled trenches." *Journal of Geotechnical Engineering*, ASCE, Vol. 117, No. 1, pp. 67-68, DOI: 10.1061/(ASCE) 0733-9410 (1991)117:1(67).

Al-Hussaini, T. M. and Ahmad, S. (1996). "Active isolation of machine foundations by in-filled trench barriers." *Journal of Geotechnical Engineering*, Vol. 122, pp. 288-294, DOI: 10.1061/(ASCE)0733-9410(1996)122:4(288).

Alpan, I. (1970). "The geotechnical properties of soils." *Earth-Science Reviews*, Vol. 6, No. 1, pp. 5-49, DOI: 10.1016/0012-8252(70) 90001-2.

Alzawi, A. and El-Naggar, M. H. (2009). "Vibration scattering using geofoam material as vibration wave barriers." *GeoHalifax, 52nd Canadian Geotechnical Conference*.

Alzawi, A. and El-Naggar, M. H. (2011). "Full scale experimental study on vibration scattering using open and in-filled (GeoFoam) wave barriers." *Soil Dynamics and Earthquake Engineering*, Vol. 31, pp. 306-317, DOI: 10.1016/j.soildyn.2010.08.010.

ASTM D6817-06 (2006). "Standard specification for rigid cellular

polystyrene geofoam." *American Society of Testing and Materials*, West Conshohocken, Pennsylvania, USA.

Babu, G. L. S., Srivastava, A., Rao, K. S. N., and Venkatesha, S. (2011). "Analysis and design of vibration isolation system using open trenches." *International Journal of Geomechanics*, Vol. 11, No. 5, pp. 364-369, DOI: 10.1061/(ASCE) GM.1943-5622.0000103.

Beskos, D. E., Dasgupta, B., and Vardoulakis, I. G. (1986). "Vibration isolation using open or filled trenches." *Computational Mechanics*, Vol. 1, No. 1, pp. 43-63, DOI: 10.1007/BF00298637.

Celebi, E. and Schmid, G. (2005). "Investigations on ground vibration induced by moving loads." *Engineering Structures*, Vol. 27, No. 14, pp. 1981-1998, DOI: 10.1016/j.engstruct.2005.05.011.

Celebi, E., Firat, S., Beyhan, G., Cankaya, I., Vural, I., and Kirtel, O. (2009). "Field experiments on wave propagation and vibration isolation using wave barriers." *Soil Dynamics and Earthquake Engineering*, Vol. 29, No. 5, pp. 824-833, DOI: 10.1016/j.soildyn.2008.08.007.

Dasgupta, B., Beskos, D. E., and Vardoulakis, I. G. (1990). "Vibration isolation using open or filled trenches, Part 2:3-D homogeneous soil." *Computational Mechanics*, Vol. 6, No. 2, pp.129-142.

Davies, M. C. R. (1994). "Dynamic soil-structure interaction resulting from blast loading." In: *Proceedings of the International Conference on Centrifuge Modelling* (Centrifuge 94), pp. 319-324.

Di Mino, G., Gunta, M., and Di Liberto, C. M. (2009). "Assessing the open trenches in screening railway ground-vibrations by means of artificial neural network." *Advances in Acoustics and Vibration*, Vol. 2009, Article ID 942787, DOI: 10.1155/2009/942787.

Duncan, J. M. and Chang, C. Y. (1970). "Nonlinear analysis of stress and strain in soils." *Journal of Soil Mechanics and Foundation Divisions*, Vol. 5, pp. 1629-1653.

Ekanayake, S. D., Liyanapathirana, D. S., and Leo, C. J. (2014). "Attenuation of ground vibrations using in-filled wave barriers." *Soil Dynamics and Earthquake Engineering*, Vol. 67, pp. 290-300, DOI: 10.1016/j.soildyn. 2014.10.004.

Haupt, W. A. (1981). "Model tests on screening of surface waves." *Proceedings of 10th International Conference of Soil Mechanics and Foundation Engineering*, Stockholm, Vol. 3, pp. 215-222.

Janbu, N. (1963). "Soil compressibility as determined by oedometer and triaxial tests." *European Conference on Soil Mechanics and Foundation Engineering*, Wissbaden, Germany, Vol. 1, pp. 19-25.

Kattis, S. E., Polyzos, D., and Beskos, D. E. (1999). "Modelling of pile barriers by effective trenches and their screening effectiveness." *Soil Dynamics and Earthquake Engineering*, Vol. 18, No. 1, pp. 1-10, DOI: 10.1016/S0267-7261(98) 0032-3.

Kramer, S. L. (1996). "Geotechnical earthquake engineering." *Prentice-Hall International Series in civil Engineering and Engineering Mechanics*, Prentice-Hall, New Jersey.

Kumar, J. and Ghosh, P. (2006). "Seismic bearing capacity for embedded footings on sloping ground." *Geotechnique*, Vol. 56, No. 2, pp. 133-140.

Liao, S. and Sangrey, D. A. (1978). "Use of piles as isolation barriers." *Journal of Geotechnical Engineering Divisions*, ASCE, Vol. 104, No. 9, pp. 1139-1152.

Lysmer, J. and Kuhlmeyer, R. L. (1969). "Finite dynamic model for infinite media." *Journal of the Engineering Mechanics Division*, ASCE, Vol. 95, pp.859-877.

Majumder, M., and Ghosh, P. (2014). "Finite element analysis of vibration screening techniques using EPS geofoam." *In Proceedings of 14th International Conference of the International Association for Computer Mechanics and Advances in Geomechanics (14th IACMAG)*, September 22-25, 2014, Kyoto, Japan.

Massarsch, K. R. (2005). "Vibration isolation using gas-filled cushions." *Soil Dynamics Symposium to Honor Prof. Richard D. Woods (Invited paper)*, *Geo-Frontiers*, Austin, Texas, January 24-26, 22.

Murillo, C., Thorel, L., and Caicedo, B. (2009). "Feasibility of the spectral analysis of surface waves technique to evaluate the shear wave velocity in centrifuge models." *Journal of Applied Geophysics*, Vol. 68, pp. 135-145, DOI: 10.1016/j.jappgeo.2008.10.007.

Nainegali, L. S. (2013). "Finite element analysis of two symmetric and asymmetric interfering footings resting on linearity and non-linearity elastic foundation beds." *PhD Thesis*, Indian Institute of Technology, Kanpur, India.

Phuoc, D. H. (2008). "Excavation behaviour and adjacent building response analyses using User Defined Soil Models in PLAXIS." *Master Thesis*, NTUST- Taiwan Tech, Taiwan.

PLAXIS 2-D –Version 8.5 (2002). "Geotechnical code for soil and rock analysis." *User's Manual, Brinkgreev, R.B.J. ed., A.A., Balkema Publishers*, Netherlands.

Richart, F., Hall, J., and Woods, R. (1970). "Vibration of soils and foundations." *Prentice Hall*, Englewood Cliffs, NJ.

Saikia, A. and Das, U. K. (2014). "Analysis and design of open trench barriers in screening steady-state surface vibrations." *Earthquake Engineering and Engineering vibrations*, Vol. 13, No. 3, pp. 545-554, DOI: 10.1007/s11803-014-0261-x.

Segol, G., Lee, P. C. Y., and Abel, J. R. (1978). "Amplitude reduction of surface waves by trenches." *Journal of the Engineering Mechanics Division*, ASCE, Vol. 104, No. 3, pp. 621-641.

Shen, C., Bang, S., and Hermann, L. (1981). "Ground Movement analysis of Earth Support system." *Journal of the Geotechnical Engineering*, ASCE, Vol. 107, No. 12, pp.1609-1624.

Tsai, P. H., Feng, Z., and Jen, T. (2008). "Three-dimensional analysis of screening effectiveness of hollow pile barriers for foundation induced vertical vibration." *Computer and Geotechnics*, Vol. 35, No. 3, pp.489-499, DOI: 10.1016/j.compgeo.2007.05.010.

Valliappan, H. S. and Murti, V. (1984). "Finite element constraints in the analysis of wave propagation problems." *UNICIV Rep. No. R-218, School pf Civil Engineering*, University of New South Wales, New South Wales, Australia.

Wang, J. G., Sun, W., and Anand, S. (2009). "Numerical investigation on active isolation of ground shock by soft porous layers." *Journal of Sound and Vibration*, Vol. 321, pp. 492-509, DOI: 10.1016/ j.jsv.2008.09.047.

Wang, Z. L., Li, Y. C., and Wang, J. C. (2006). "Numerical analysis of attenuation effect of EPS geofoam on stress waves in civil defense engineering." *Geotextiles and Geomembranes*, Vol. 24, No. 5, pp. 265-273, DOI: 10.1016/j. geotexmen. 2006.04.002.

Woods, R. (1968). "Screening of surface waves in soils." *Journal of Soil Mechanics and Foundations*, Vol. 94, pp. 951-979.